

Article

Spatiotemporal Dynamics and Lagged Hydrological Impacts of Compound Drought and Heatwave Events in the Poyang Lake Basin

Ningning Li ^{1,2}, Yang Yang ³, Zikang Xing ^{4,*}, Yi Zhao ³, Jianhui Wei ⁵, MiaoMiao Ma ⁶ and Xuejun Zhang ⁶

¹ Engineering Geology Brigade of Jiangxi Bureau of Geology, Nanchang 330001, China; 2023110051@ecut.edu.cn

² School of Earth and Planetary Sciences, East China University of Technology, Nanchang 330013, China

³ Geological Environment Monitoring Institute of Jiangxi Geological Survey and Exploration Institute, Nanchang 330006, China

⁴ State Key Laboratory of Lake and Watershed Science for Water Security, Nanjing Institute of Geography and Limnology, Chinese Academy of Sciences, Nanjing 211135, China

⁵ Institute of Meteorology and Climate Research (IMK-IFU), Karlsruhe Institute of Technology, Campus Alpin, 82467 Garmisch-Partenkirchen, Germany

⁶ Research Center on Flood and Drought Disaster Reduction of the Ministry of Water Resources, China Institute of Water Resources and Hydropower Research, Beijing 100038, China

* Correspondence: zkx@niglas.ac.cn

Abstract

Compound drought and heatwave (CDHW) events pose a rising threat to global water security and ecosystem stability. While their increased frequency under global warming is recognized, their spatiotemporal evolution and subsequent cascading impacts on hydrological processes in monsoonal lake basins remain poorly quantified. This study investigates the characteristics and hydrological impacts of CDHW in the Poyang Lake Basin, China's largest freshwater lake, from 1981 to 2016. Using a daily rolling-window approach with the Standardized Precipitation Index (SPI) and Standardized Temperature Index (STI), we identified CDHW events and characterized them with metrics of frequency, severity, and intensity. Event coincidence analysis (ECA) was employed to quantify the trigger relationship between CDHW and subsequent hydrological droughts (streamflow and lake water level). Our results reveal a paradigmatic shift in the CDHW regime post-2000, marked by statistically significant increases in all three metrics and a fundamental alteration in their statistical distributions. ECA demonstrated that intensified CDHW events significantly enhance hydrological drought risk, primarily through a robust and increasing lagged influence at seasonal timescales (peaking at 40–90 days). Decomposition of compound events attributes this protracted impact predominantly to the heatwave component, which imposes prolonged hydrological stress, in contrast to the more immediate but rapidly decaying influence of drought alone. This study highlights the necessity of integrating compound extremes and their non-stationary, lagged impacts into water resource management and climate adaptation strategies for monsoonal basins.



Academic Editor: Andrzej Walega

Received: 17 November 2025

Revised: 19 December 2025

Accepted: 25 December 2025

Published: 30 December 2025

Copyright: © 2025 by the authors.

Licensee MDPI, Basel, Switzerland.

This article is an open access article distributed under the terms and conditions of the [Creative Commons Attribution \(CC BY\) license](#).

Keywords: compound extreme; drought; heatwave; Poyang Lake Basin; hydrological impact; event coincidence analysis

1. Introduction

Compound drought and heatwave (CDHW) events have become a rising concern due to their widespread impacts on socio-ecological systems [1,2]. These events pose serious

threats, including increased wildfires, heat-related mortality, and agricultural losses [3]. The evolution of CDHW is driven by complex land–atmosphere interactions, while their spatial patterns exhibit considerable heterogeneity across regions, influenced by local variations in precipitation, temperature anomalies, and other hydrological factors [4,5].

Over the past decades, observational records and climate model projections have consistently shown a significant increase in the frequency and intensity of CDHW across global land areas [6,7]. This trend is particularly pronounced in East Asian monsoon regions like eastern China, where rapid warming and changing atmospheric circulation patterns have created favorable conditions for the concurrence of drought and heat extremes [8,9]. The accelerated warming observed since the late 20th century has further amplified this trend, making CDHW one of the most concerning climate threats in densely populated monsoon regions [10].

The increasing frequency of CDHW poses substantial threats to hydrological systems and water security [11]. These compound events can lead to more severe reductions in streamflow and lake water levels than individual extremes, significantly exacerbating hydrological droughts [12]. Recent analyses further suggest that the synergistic effects of concurrent droughts and heatwaves often result in impacts that are disproportionate to the sum of their individual parts, challenging existing risk assessment frameworks [13]. During CDHW, the combined stress of precipitation deficit and excessive evaporative demand creates a double burden on water resources, potentially leading to earlier onset, longer duration, and more severe hydrological droughts [14]. This is particularly critical for water resource management as the compounding effects can overwhelm traditional drought preparedness systems designed based on historical, single-hazard events [15].

Various methodologies have been employed to analyze CDHW events and their impacts, including statistical approaches and dynamical modeling. For example, the logistic regression model and partial correlation were used to systematically quantify the combined influence of major teleconnection patterns and anthropogenic warming on global CDHW [7]. By applying a novel copula-based approach to CMIP6 multi-model ensembles, Bastien and Mathieu [16] assessed the time of emergence for CDHW and revealed that both shifting marginal properties and dependence structure are key, yet highly variable, drivers of future risk. Wang et al. [17] revealed that CDHW events intensify more rapidly in drylands than in humid regions, with heatwaves being the dominant driver in drylands, whereas droughts prevail in humid areas. Among these methods, traditional correlation analyses [18] and Copula functions [19] have been widely applied to identify long-term changes in compound events. However, these conventional approaches often fail to capture the temporal dependencies and lagged responses between climate extremes and hydrological impacts. Hence, Event-based Coincidence Analysis (ECA) has recently emerged as a powerful tool for quantifying the synchronized occurrence of discrete events across different temporal scales [20,21], offering new opportunities to understand the lagged hydrological impacts of CDHW.

The Poyang Lake Basin (PLB) provides an ideal natural laboratory for studying CDHW impacts on monsoon freshwater systems. As China's largest freshwater lake, Poyang Lake supports critical ecosystem services and socioeconomic development in the Yangtze River region [22]. The basin's humid subtropical monsoon climate, characterized by strong seasonality and considerable interannual variability, makes it particularly vulnerable to compound events [23]. Previous studies in the PLB have documented increasing trends in both drought and heatwave events separately, and their severe impacts on lake hydrology and ecology [24,25]. However, a systematic investigation of CDHW and their lagged effects on both river flow and lake level dynamics remains lacking, limiting our understanding

of how compound extremes propagate through the watershed and affect the integrated river-lake system.

In this study, CDHW events are identified using a daily rolling-window approach that integrates the Standardized Precipitation Index (SPI) [26] and the Standardized Temperature Index (STI) [27]. The SPI is a widely adopted metric for characterizing meteorological drought based on precipitation anomalies. We employ the STI as a directly analogous index for temperature. This methodological symmetry ensures that the drought and heatwave components are quantified on a consistent, probabilistic scale, facilitating the direct comparison and combination of precipitation deficits and temperature excesses to define concurrent extremes [28].

This study aims to address these research gaps by conducting a comprehensive analysis of CDHW characteristics and their hydrological impacts in the PLB from 1981 to 2016. Specifically, we seek to (1) quantify the spatiotemporal evolution of CDHW and identify potential regime shifts, (2) analyze the lagged effects of CDHW on streamflow and lake water level using Event coincidence analysis, and (3) assess the sensitivity of hydrological responses to CDHW severity. Our findings will provide valuable insights into water resource management and climate adaptation in monsoonal lake basins facing increasing compound extreme events.

2. Materials and Methods

2.1. Study Area

The Poyang Lake Basin ($24^{\circ}29' - 29^{\circ}42' \text{ N}$, $113^{\circ}34' - 118^{\circ}36' \text{ E}$, Figure 1) spans approximately $162,000 \text{ km}^2$ in Jiangxi Province, southern China [29]. As China's largest freshwater lake, Poyang Lake plays a critical role in regional hydrology, ecology, and socio-economic development [30]. The basin experiences a humid subtropical monsoon climate with distinct seasonal variations, characterized by a mean annual precipitation of $1500 - 1700 \text{ mm}$ and mean annual temperature of $17 - 18^{\circ}\text{C}$ [31]. The highly dynamic lake surface area (ranging from $\sim 1000 \text{ km}^2$ in dry season to $>3000 \text{ km}^2$ in wet season) and complex river-lake interactions make it particularly sensitive to compound extreme events [32].

2.2. Data Sources

This study integrates multi-source observational and reanalysis datasets encompassing meteorological, hydrological, and limnological variables to comprehensively investigate the CDHW events and their hydrological impacts in the Poyang Lake basin. The detailed data sources and characteristics are summarized in Table 1.

Meteorological data were obtained from two complementary sources to ensure comprehensive spatial coverage and data reliability. Daily maximum temperature and precipitation records were acquired from 27 meteorological stations operated by the China Meteorological Administration (CMA). To enhance spatial resolution and provide continuous gridded coverage, we supplemented station observations with the ERA5-Land reanalysis dataset [33], which provides daily meteorological variables at a high spatial resolution of $0.1^{\circ} \times 0.1^{\circ}$ and were bias-corrected using the Quantile Mapping method against the station observations [34]. Both datasets cover the 36-year study period from 1980 to 2023.

Hydrological data were collected from the Jiangxi Hydrological Bureau, encompassing both river discharge and lake level measurements. River runoff data were obtained from 7 gauging stations strategically located along the five major tributaries of Poyang Lake. Daily water level elevation records were acquired from 5 primary lake level stations situated in Poyang Lake. All hydrological measurements were recorded at daily intervals throughout the 1981–2016 study period.

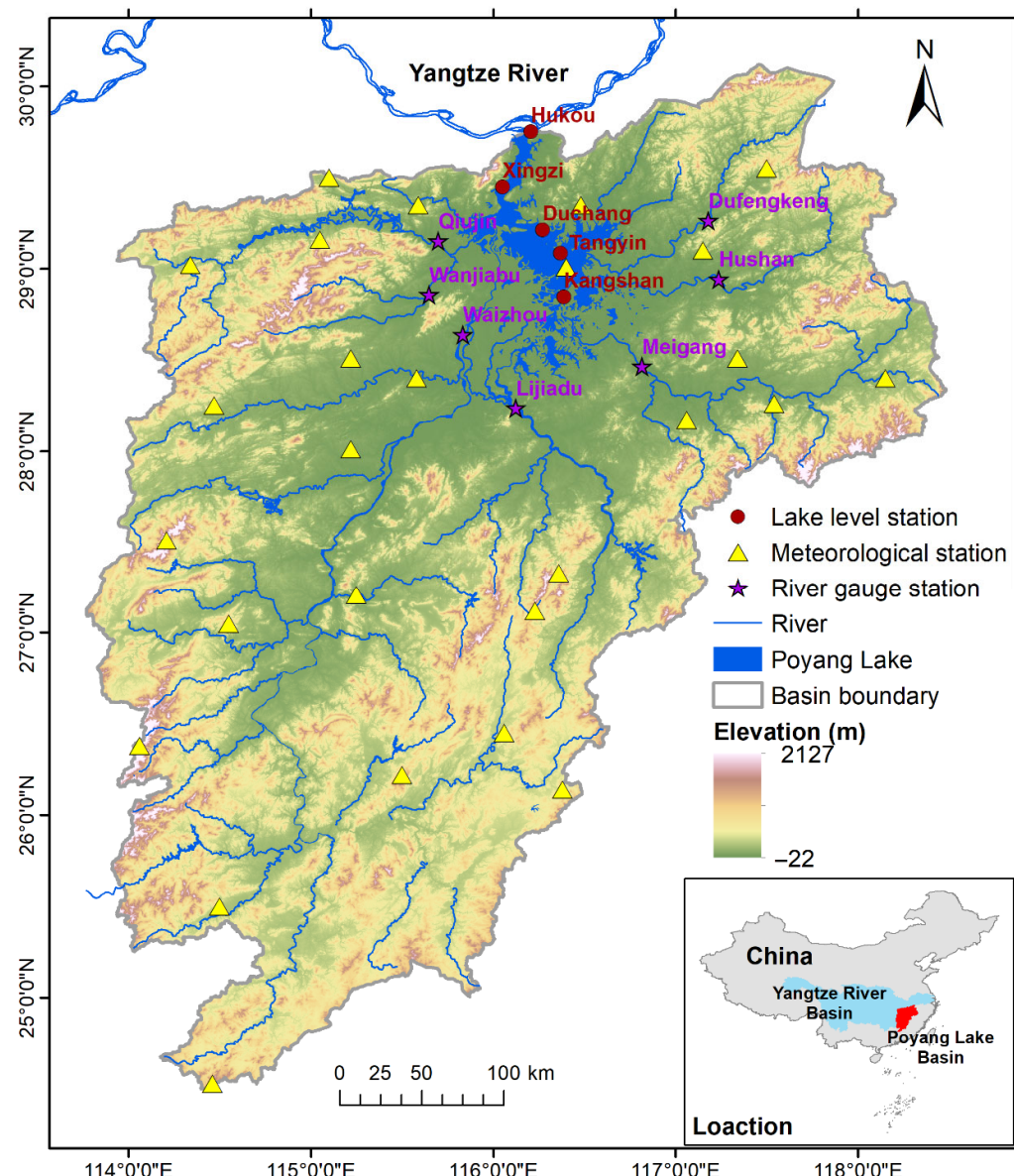


Figure 1. Geographic features of the PLB and location of the meteorological, river gauge and lake level stations in the basin.

Table 1. Data sources and characteristics.

Data Type	Source	Spatial Resolution	Temporal Resolution	Time Period	Variables Used
Reanalysis Data	ERA5-Land	$0.1^\circ \times 0.1^\circ$	Daily	1980–2023	Maximum temperature, precipitation
Meteorological stations	China Meteorological Administration	27 stations	Daily	1980–2023	Maximum temperature, Precipitation
River gauge stations	Jiangxi Hydrological Bureau	5 major tributaries (7 stations)	Daily	1981–2016	Runoff discharge
Lake Level stations	Jiangxi Hydrological Bureau	5 main stations	Daily	1981–2016	Water level elevation

2.3. Methods

2.3.1. Definition of Compound Drought and Heatwave Event

CDHW events were identified using a daily rolling-window methodology that integrates concurrent meteorological drought and extreme heat conditions. Drought intensity was characterized by the 90-day Standardized Precipitation Index (SPI) [26], with daily index values derived from precipitation accumulations over the preceding 90-day period.

Concurrently, extreme heat was quantified by the 90-day Standardized Temperature Index (STI) [35], computed from daily maximum temperatures over an identical moving window to ensure temporal consistency. A CDHW event was defined as a period where daily SPI fell below -0.5 , indicating dry conditions, while daily STI simultaneously exceeded 1 , signifying anomalously high temperatures, for at least three consecutive days [2]. The threshold of $\text{SPI} < -0.5$ is commonly used to define meteorological drought conditions in compound event studies [36,37], representing a dry anomaly (approximately the 30th percentile). This threshold is chosen to ensure consistency with the moderate heat anomaly defined by $\text{STI} > 1.0$ (~84th percentile) and to retain a sufficient number of events for robust statistical analysis, particularly for the subsequent event-based coincidence analysis.

The adoption of SPI and STI is motivated by their key advantages in climate extreme analysis. As standardized probability indices, they transform the original precipitation and temperature data into a Gaussian distribution, which effectively eliminates the influence of geographic and seasonal disparities [38]. This normalization process facilitates direct comparison across different climatic regions and seasons and is particularly suited for identifying relative extremes in a daily rolling assessment [39]. Computationally, both indices follow the same core procedure: for each calendar day, a 90-day window centered on that day across all years forms the sample for fitting a probability distribution (e.g., Gamma for precipitation, Gaussian for temperature). The fitted distribution is then transformed to a standard normal distribution, yielding the daily index value where negative SPI indicates dryness and positive STI indicates warmth. The adoption of a 90-day window for the SPI and STI is aligned with the climatological regime of the PLB, which is dominated by a pronounced East Asian monsoon climate [40]. This climate is characterized by strong seasonal cycles in both precipitation and temperature. The 90-day scale effectively captures seasonal moisture deficits associated with monsoon dynamics, which are critical drivers of streamflow and lake level variations. This approach allows us to investigate how sub-seasonal to seasonal compound stress (heatwaves superimposed on seasonal drought) propagates into the hydrological system with lags of weeks to months. While shorter scales like SPI-30 are excellent for characterizing short-term agricultural or soil moisture drought, they are less representative of the moisture status that governs seasonal river discharge and lake water storage. Our time scale choice is consistent with studies focusing on the hydrological impacts of compound events in monsoon regions [41,42].

Three key metrics were employed to characterize the events: frequency, severity, and intensity. Frequency was defined as the total number of days experiencing CDHW conditions within a given period (monthly or yearly), expressed as a percentage of the total days in that period. Severity was calculated as the cumulative magnitude of the compound phenomenon, represented by the sum of the products of the absolute values of the corresponding daily SPI and STI throughout all CDHW days within the period of interest. Intensity was determined as the ratio of severity to frequency within a certain period, providing a measure of the average compound impact per event day. This multi-metric framework allows for a comprehensive quantification of the occurrence, magnitude, and average strength of compound extremes.

To quantify and compare the contributions of individual components within compound events, this study also extracted two types of independent extreme events for comparative analysis: (1) Standalone drought events, defined as periods meeting $\text{SPI} < -0.5$ and $\text{STI} < 1$; (2) Standalone heatwave events, defined as periods meeting $\text{STI} > 1$ and $\text{SPI} > -0.5$. These definitions ensure that the standalone events are mutually exclusive with the compound events ($\text{SPI} < -0.5$ and $\text{STI} > 1$).

2.3.2. Definition of Streamflow Drought and Lake Water Drought

To quantitatively assess the hydrological responses to CDHW and maintain methodological consistency with the meteorological drought indices, standardized indices were also employed for characterizing streamflow and lake water level anomalies. Streamflow drought was defined using the Standardized Runoff Index (SRI) [43]. The SRI was calculated on a daily basis for each hydrological station using a 90-day rolling window of daily streamflow data. This process, analogous to the SPI calculation, transforms the raw streamflow series into a standardized Gaussian distribution, enabling the identification of periods of anomalously low runoff relative to the historical distribution for the same time of year. Similarly, lake water drought was characterized by the Standardized Water-level Index (SWI). The daily SWI was derived by applying the same standardization procedure to the 90-day rolling window of daily lake water level records from each monitoring station.

2.3.3. Trend Analysis

Theil-Sen trend [44] was employed to examine the temporal evolution of CDHW event characteristics, including frequency, intensity, and duration. Theil-Sen analysis is a robust, nonparametric statistical method that estimates the magnitude of trends by computing the median of all possible pairwise slopes within the time series.

To investigate the potential influence of accelerated climate warming on CDHW dynamics, we conducted trend analyses separately for two distinct climatic periods: a baseline period (pre-2000; 1980–1999) and a recent warming period (post-2000; 2000–2023). The selection of the year 2000 as a breakpoint is supported by both regional climatic shifts and statistical validation. Firstly, this division aligns with a documented acceleration in global and regional warming rates around the turn of the century, with the post-2000 period in our study basin exhibiting consistently positive summer temperature anomalies of 0.5–0.75 °C relative to the 1980–1999 mean [2,38]. Secondly, to objectively confirm a shift in the CDHW regime, we applied a change point model (CPM) [45] to the annual series of CDHW intensity. The test identified a statistically significant ($p < 0.05$) change point in the year 2000, validating our temporal division [46]. The bipartite analysis enables the detection of non-stationary behavior and facilitates the attribution of observed changes to recent warming intensification [47].

2.3.4. Event-Based Coincidence Analysis

Event-based Coincidence Analysis (ECA), developed by Donges et al. (2016) [20] and Siegmund et al. (2017) [21], is specifically designed to assess the inter-dependency between discrete event series by quantifying their synchronized occurrences within defined temporal windows. ECA has been successfully applied across diverse hydro climatological contexts, including flood-epidemiology linkages, extreme event timing, and drought propagation studies [48–50].

In this study, we applied ECA to examine the temporal linkages between CDHW events and hydrological responses, including both river discharge and lake water level. CDHW events were defined when the CDHW intensity index exceeded zero, while hydrological drought events were identified when either the SRI or SWI fell below -0.5 . We focused on the trigger coincidence rate (TCR), which quantifies the proportion of hydrological drought events that are preceded by CDHW events within a specified temporal window. The TCR is mathematically expressed as:

$$TCR = \frac{1}{N_A} \sum_{i=1}^{N_A} \Theta \left(\sum_{j=1}^{N_B} 1_{[\tau, \tau + \Delta T]} (t_A^i - t_B^j) \right) \quad (1)$$

where t_A^i and t_B^j represent the occurrence times of hydrological drought events (A-type) and CDHW events (B-type), respectively; τ denotes the lag time between event types; ΔT defines the coincidence window duration; $\Theta(\cdot)$ is the Heaviside function; and $1_I(\cdot)$ is the indicator function for interval I. The analysis incorporated a lag range of 0–91 days to capture the spectrum of hydrological response timescales. A coincidence window (ΔT) of 5 days was selected to accommodate timing uncertainties. A 5-day coincidence window was selected following precedent in Event Coincidence Analysis studies [51,52]. This duration accommodates potential uncertainties in the exact timing of hydrological responses to atmospheric extremes while minimizing the over-smoothing of lag-specific relationships that might occur with a longer window.

To investigate the intensifying effect of recent warming on CDHW-hydrology relationships, we conducted separate ECA for pre-2000 (1981–1999) and post-2000 (2000–2016) periods. This bipartite temporal framework enables the detection of non-stationarities in coincidence patterns and facilitates attribution to climate warming. The statistical significance of observed coincidence rates was evaluated using Poisson process-based testing, which assesses whether the temporal clustering of events exceeds random expectations.

3. Results

3.1. Spatiotemporal Trends of CDHW

The spatiotemporal patterns of CDHW events across the Poyang Lake Basin from 1980 to 2023 are delineated in Figure 2. Over the study period, the PLB exhibited pronounced and statistically significant increasing trends in all three characteristics of CDHW events. The frequency of CDHW increased at a rate of 0.44% per year, while the severity and intensity rose by 0.8 and 0.02 per year, respectively. Spatially, the CDHW metrics displayed a notable meridional distribution pattern, characterized by higher values in the central latitudinal zones and lower values in the northern and southern parts of the basin. Specifically, the frequency and severity were more pronounced in the eastern and western sectors of the basin. In contrast, the intensity was elevated primarily in the central region, as well as the northeastern and northwestern areas. The spatial heterogeneity in CDHW is likely influenced by a combination of local factors. These include differences in topography and land cover, with the southern regions being more mountainous, as well as the modulating effect of the lake on local temperature and moisture conditions in the central and northern areas.

To investigate the potential contribution of recent warming, the interannual trends in CDHW were compared between the historical baseline period (1981–1999) and the recent warmer period (2000–2023). Our analysis reveals a marked intensification of CDHW events in the post-2000 period. The mean values of CDHW frequency, severity, and intensity post-2000 were 3.2%, 12.1, and 0.43, respectively, representing an increase by factors of 2.8, 3.0, and 2.4 compared to the pre-2000 period. This dramatic surge was largely driven by several exceptionally extreme years, namely 2003, 2006, 2009, 2013 and 2022, all of which are documented in the literature as periods of severe drought. It is noteworthy that CDHW occurred almost every year after 2000 (except for 2002), and the magnitude of these events consistently and substantially exceeded those observed in the pre-2000 era. In stark contrast, CDHW events were identified in only 63% of the years during the pre-2000 period. This clear regime shift provides strong evidence that recent climate warming has significantly amplified the occurrence, magnitude, and overall threat of CDHW events in the basin.

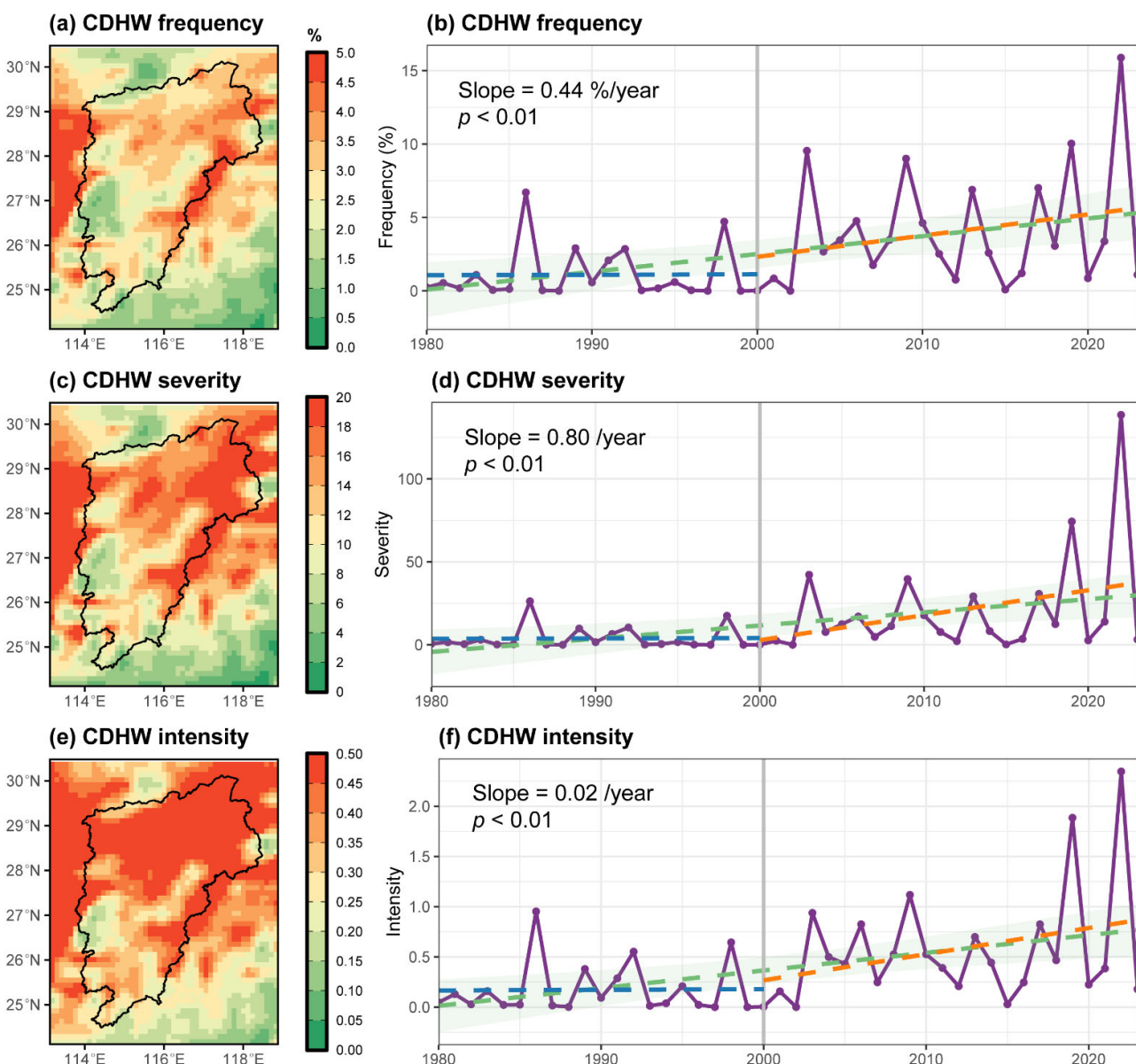


Figure 2. Spatial patterns and temporal evolution of CDHW characteristics across the Poyang Lake Basin during the study period. (a,c,e) Spatial distribution of average CDHW frequency, severity, and intensity. (b,d,f) The corresponding interannual variability (purple lines) and temporal trend for the entire period (1980–2023, green dashed line), the pre-2000 period (1980–1999, blue dashed line), and the post-2000 period (2000–2023, orange dashed line). The grey shaded areas represent the 95% confidence interval for the trend of the entire period. The grey lines represent the location of year 2000.

A comparative analysis of the pre- and post-2000 periods reveals a pronounced intensification and a fundamental shift in the statistical distribution of CDHW events across the basin. The spatial pattern of the change ratio (post-2000 mean/pre-2000 mean) demonstrates that the amplification of CDHW was not uniform (Figure 3a,c,e). The most dramatic increases, with ratios reaching 6 to 8 times the pre-2000 levels, were concentrated in the northeastern and northwestern parts of the basin. In contrast, the southern regions exhibited a more moderate, yet substantial, amplification of approximately 2-fold.

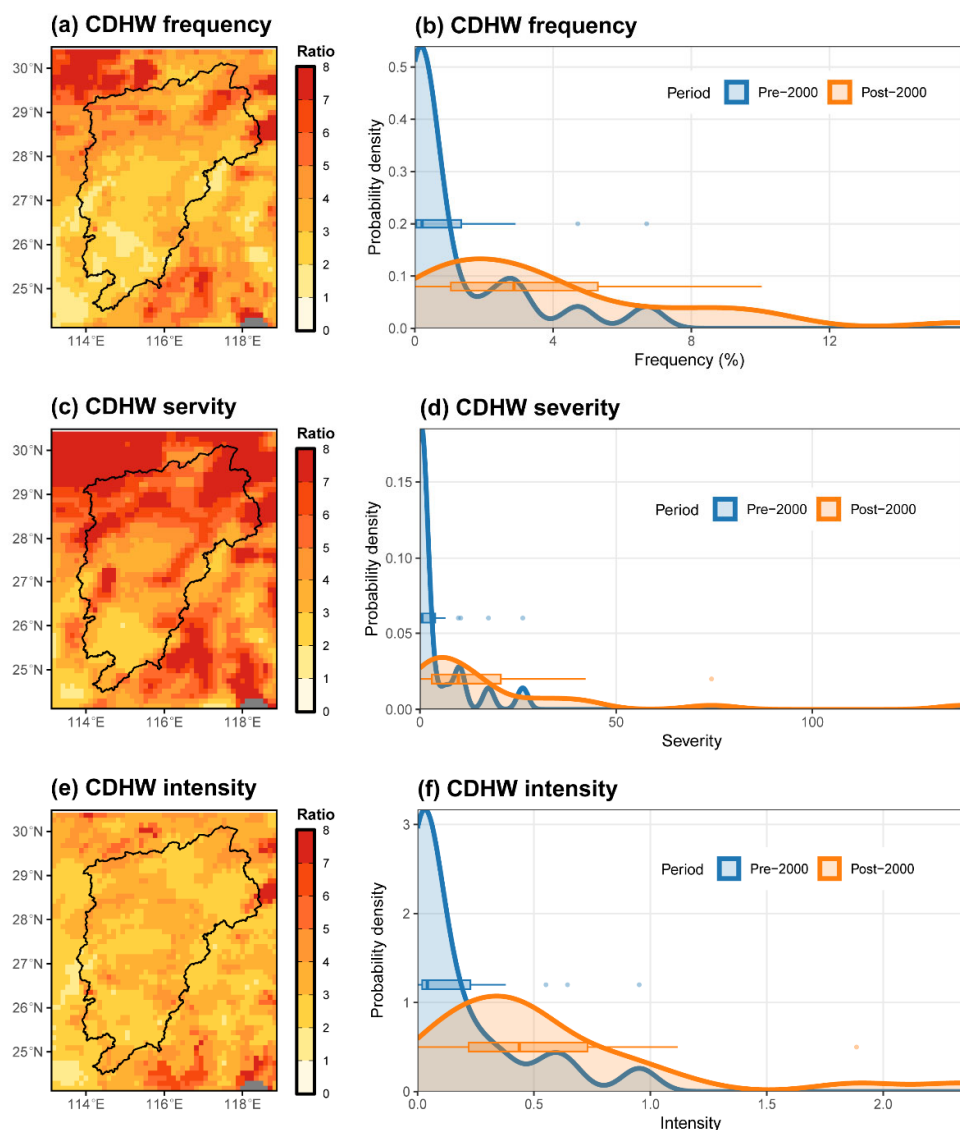


Figure 3. Changes in CDHW characteristics between the pre-2000 and post-2000 periods. (a,c,e) Spatial distribution of the change ratio (post-2000 mean/pre-2000 mean) for CDHW frequency, severity, and intensity, respectively. The black outline represents the Poyang Lake Basin. The gray area represents regions with no data. (b,d,f) Corresponding probability density curves and boxplots comparing the distributions of each CDHW metric between the two periods. The boxplots depict the 10th, 25th, 50th (median), 75th, and 90th percentiles. The dots represent outliers.

This intensification is further corroborated by a profound change in the frequency distributions of all CDHW metrics (Figure 3b,d,f). The summary statistics from the boxplots show that the 90th percentile values for frequency, severity, and intensity increased from 3.1%, 11.1 and 0.6 to 7.7%, 33.4, and 0.9, respectively, indicating a marked expansion of the upper extremes. More fundamentally, the entire shape of the probability density functions changed. The distributions for the pre-2000 period were heavily clustered in the lower value range. In the post-2000 period, the peaks of these density curves shifted towards higher values, the distributions became flatter (broader) and covered a wider range of values. This shift was particularly striking for CDHW intensity, where the primary peak completely relocated from around 0.1 to 0.4.

The analysis further elucidates a significant shift in the seasonal distribution of CDHW events in the PLB, a region known for its pronounced seasonality in climate extremes. As illustrated in Figure 4a–c, CDHW events during the entire study period predominantly

occurred from September to November, with the peak magnitude across all three metrics consistently observed in October.

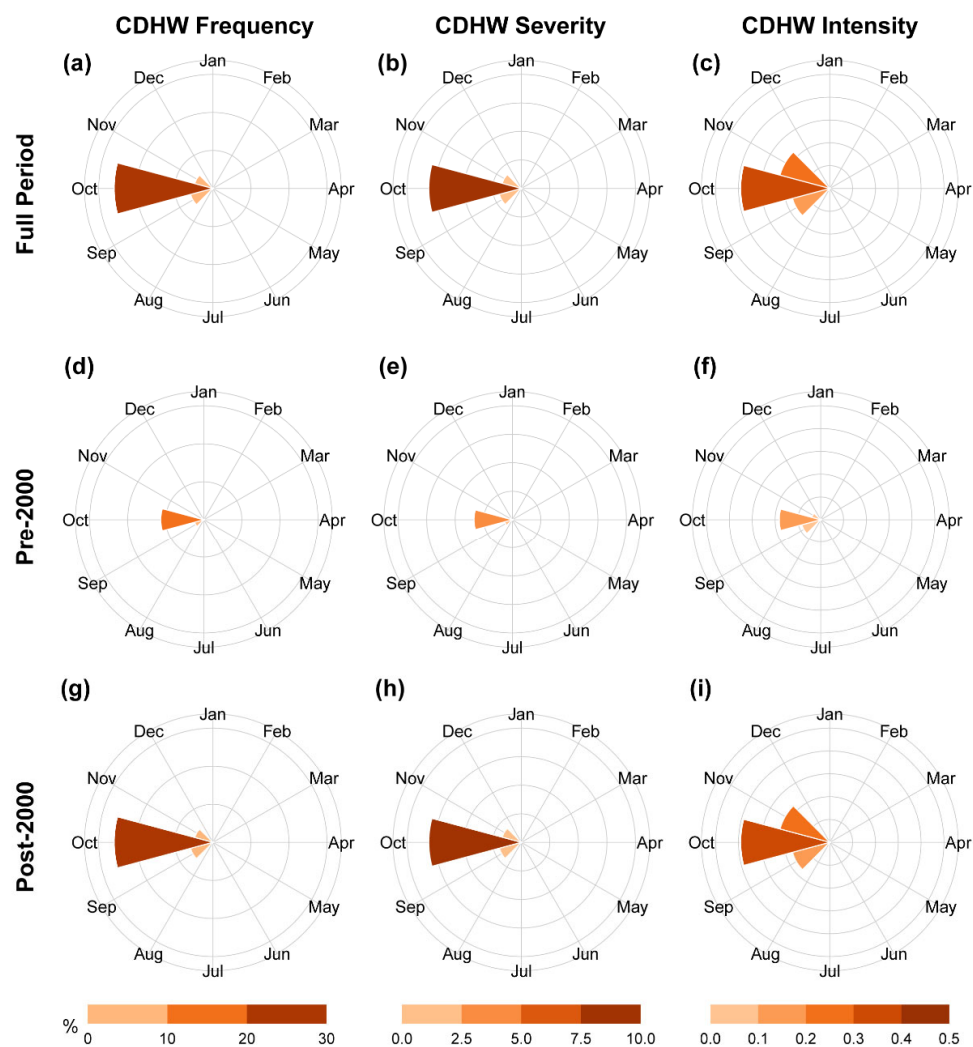


Figure 4. Seasonal patterns of CDHW characteristics in the PLB. (a–c) Monthly averages (depicted as wind rose diagrams) of CDHW frequency, severity, and intensity for the entire study period. (d–i) represent the corresponding seasonal patterns for the pre-2000 and post-2000 periods, respectively.

A comparative examination of the pre- and post-2000 epochs, however, reveals a notable evolution of this seasonal pattern. In the pre-2000 period (Figure 4d–f), while CDHW events were still largely confined to September–November, their intensity in October was relatively subdued, and events in September and November were particularly weak. In stark contrast, the post-2000 period (Figure 4g–i) is characterized by a marked amplification of autumn CDHW. Not only was the peak intensity in October substantially enhanced, but a pronounced strengthening is also evident in September and November.

These results collectively reveal a shifting seasonal regime of CDHW events before and after the year 2000. The core autumn has experienced significant intensification, with the temporal footprint of high intensity CDHW expanding from a concentrated peak in October towards a broader window encompassing both September and November. This expansion indicates that recent warming has not only amplified the intensity of compound events but has also effectively extended their favored occurrence period within the annual cycle.

3.2. Lagged Influence of CDHW on Hydrological Drought

The amplification of hydrological drought resulting from the intensification of CDHW has been quantified at a daily scale employing ECA (Figure 5). The rise in the mean trigger coincidence rate for streamflow drought and lake water drought from 0.21 and 0.05 (pre-2000) to 0.24 and 0.12 (post-2000), which represents increases of 14.3% and 140%, respectively, provides key statistical evidence that the intensified CDHW events are associated with a higher occurrence frequency of subsequent hydrological droughts. This strengthened statistical linkage can be explained by our mechanistic analysis showing the enhanced and prolonged hydrological impact of the heatwave component post-2000, thereby substantiating that the enhanced CDHW regime has become a more frequent and effective precursor to hydrological drought in the basin.

Furthermore, CDHW exerted a pronounced lagged influence on both streamflow and lake water levels, with the trigger coincidence rate increasing progressively with longer lags (Figure 5). For streamflow drought (Figure 5a), this lagged influence became markedly more robust after 2000. In the pre-2000 period, the coincidence rate curve was relatively flat, indicating a weak delayed response. Conversely, in the post-2000 period, the rate exhibited a significant upward trend with increasing lag. A critical finding is that for lags of 0–40 days, the post-2000 coincidence rate was lower than its pre-2000 counterpart. However, beyond a lag of 40 days, the relationship reversed, with the post-2000 period showing consistently higher rates. This suggests that the more intense CDHW post-2000 did not enhance the immediate runoff response but substantially strengthened the seasonal-scale, cumulative impact on streamflow depletion.

The lagged effect was even more pronounced for lake water drought (Figure 5b). In the pre-2000 period, the coincidence rate remained at zero for lags of 0–30 days, only beginning to rise gradually thereafter. In the post-2000 period, a low but immediate response (0.05) was observed at lags of 0–15 days, followed by a steep and significant increase in longer lags. Notably, for all lag times, the coincidence rate in the post-2000 period surpassed that in the pre-2000 period. As the terminal component of the atmosphere-runoff-lake hydrological cycle, the absolute coincidence rate for lake water level was lower than that for streamflow, yet its lagged response was more pronounced.

To disentangle the drivers behind the enhanced lagged hydrological impact of CDHW, we conducted a comparative ECA isolating the effects of standalone drought and standalone heatwave events.

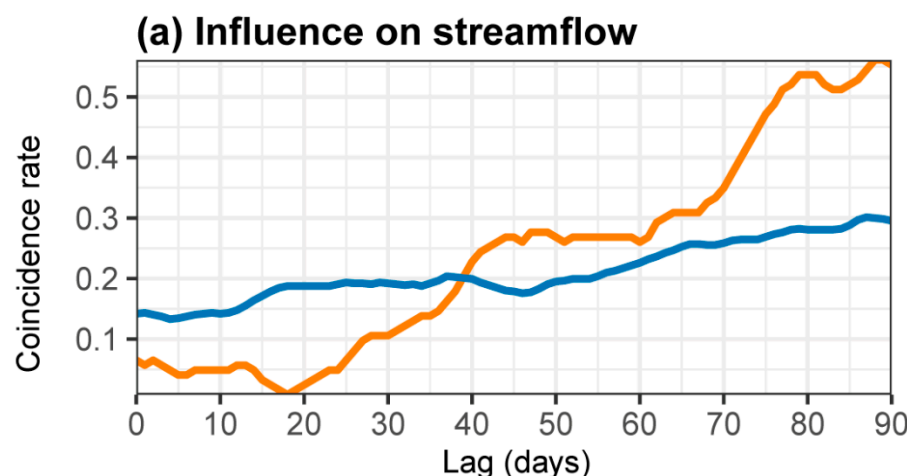


Figure 5. Cont.

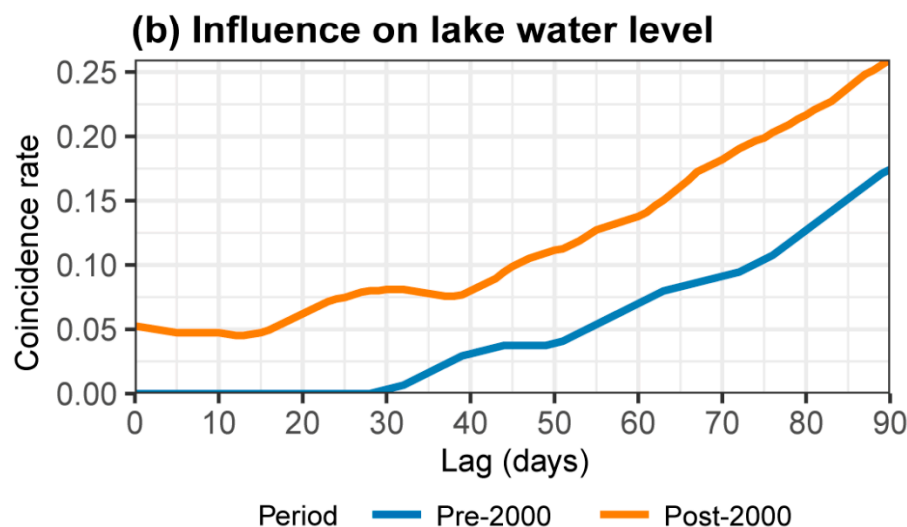


Figure 5. CDHW's influence on hydrological regimes based on ECA. The trigger coincidence rate between CDHW events and (a) streamflow drought (mean across all hydrological stations), and (b) lake water drought (mean across all lake level stations) is shown as a function of temporal lag (days) for both the pre-2000 and post-2000 periods.

For streamflow drought (Figure 6), the analysis reveals distinctly different temporal influence patterns between the two drivers. Standalone drought events exhibited a dominant immediate impact, with their influence decaying as the lag increased, in both the pre- and post-2000 periods. In stark contrast, standalone heatwaves demonstrated a much more persistent and significant lagged influence, particularly at medium- to long-term scales. This indicates that meteorological drought impacts propagate through the runoff system rapidly, while heatwaves impose more prolonged hydrological stress. Consequently, the strengthened lagged impact of CDHW on streamflow, especially post-2000, is primarily attributable to the inherent persistence of heatwave impacts on hydrological processes. The post-2000 amplification of this heatwave lagged effect directly corresponds to the enhanced lagged influence observed in CDHW. Conversely, the weaker lagged impact of CDHW in the pre-2000 period can be linked to a concurrently weaker lagged influence from standalone droughts during that period.

A similar mechanistic breakdown was identified for lake water drought (Figure 7). Standalone droughts again showed a characteristic pattern of strong immediate influence followed by a decay with increasing lag. Standalone heatwaves, however, displayed the opposite signature: a weak immediate effect but a robust and strengthening influence at longer lags. The superposition of these two patterns in a compound event results in the pronounced lagged impact characteristic of CDHW on lake levels. As with streamflow, this lagged impact is predominantly governed by the persistent hydrological signature of the heatwave component. The high trigger coincidence rate (0.8 to 1.0) for standalone drought reflects the direct and rapid propagation of precipitation deficits into the hydrological system, which is a fundamental characteristic of drought progression.

In summary, the decomposition of CDHW into their constituent parts unequivocally demonstrates that the observed increase in hydrological lagged effects is driven chiefly by the protracted nature of heatwave impacts, rather than by the more immediate effects of drought. This finding underscores a critical mechanism through which a warming climate exacerbates hydrological extremes: by extending the temporal footprint of heatwaves within compound events, thereby prolonging and intensifying water deficits in watersheds and lakes.

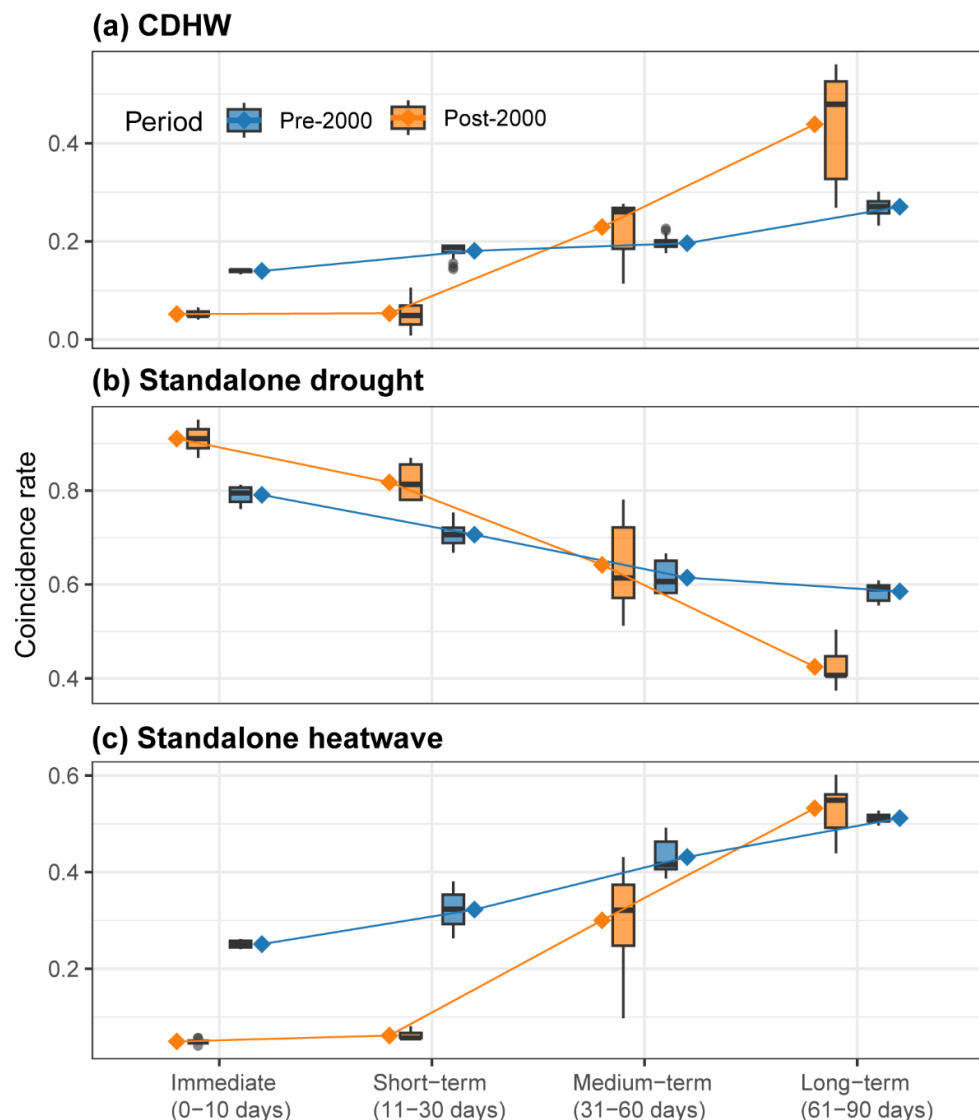


Figure 6. Comparative contribution of compound and standalone events to streamflow drought. The trigger coincidence rates for CDHW events, standalone drought (D), and standalone heatwave (HW) are summarized for immediate, short-term, medium-term, and long-term lag windows. Boxplots represent the variability of coincidence rates within each defined lag window.

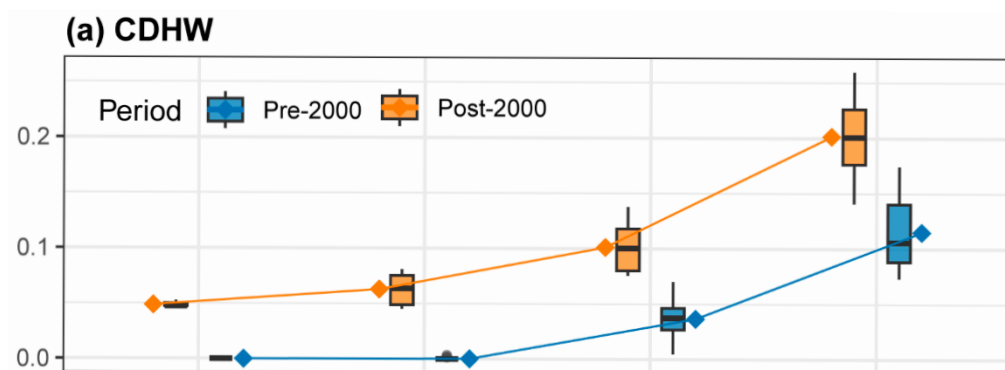


Figure 7. Cont.

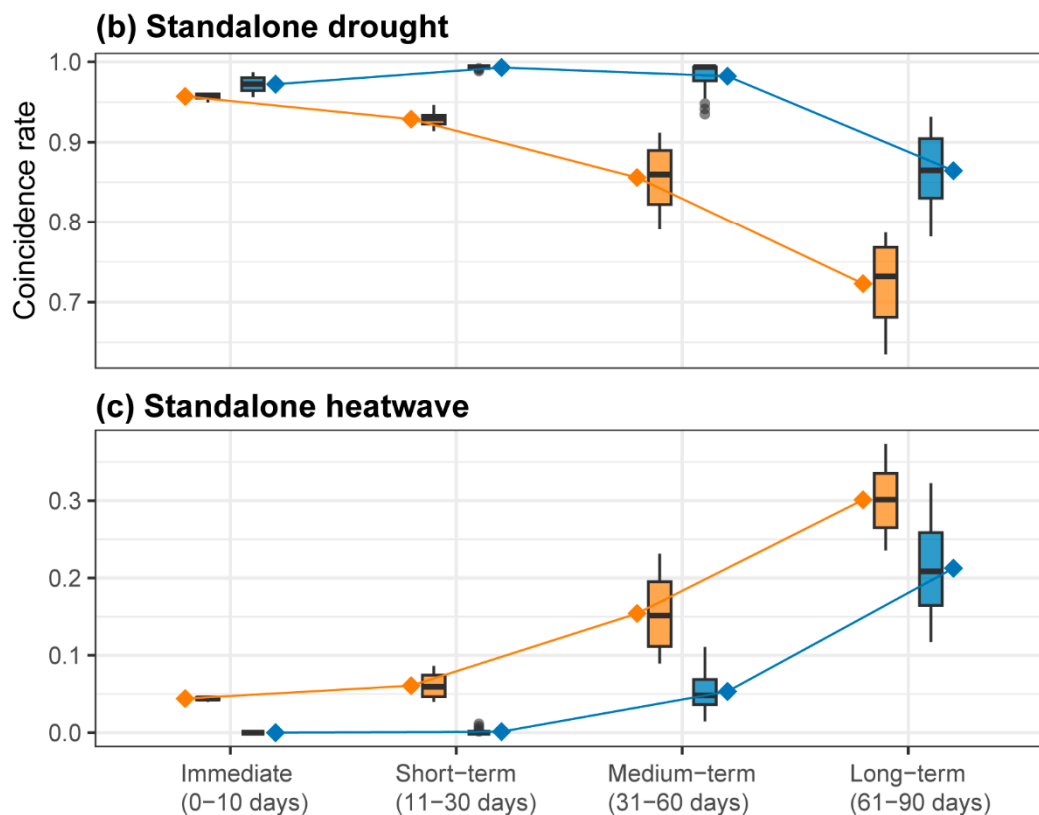


Figure 7. Comparative contribution of compound and standalone events to lake water drought. The trigger coincidence rates for CDHW events, standalone drought (D), and standalone heatwave (HW) across different lag windows. Boxplots represent the variability of coincidence rates within each defined lag window.

3.3. Sensitivity of CDHW's Influence on Hydrological Regimes

A sensitivity analysis was conducted to explore how the CDHW severity modulates their hydrological impacts by applying varying thresholds to CDHW severity. The results demonstrate that the influence of CDHW on hydrological droughts is highly sensitive to event severity. As expected, higher severity thresholds generally resulted in a lower trigger coincidence rate due to the reduced frequency of CDHW. However, across all thresholds, a significant lagged influence was consistently observed. Notably, the sensitivity to CDHW severity was more pronounced at longer lags, indicating that the intensity of a compound event primarily governs its impact on hydrological droughts at seasonal timescales, rather than immediately.

For streamflow drought (Figure 8a,b), the lagged response exhibited a bimodal structure, a feature that became markedly more distinct with increasing severity thresholds, especially in the post-2000 period. Two peak periods of influence were identified: the first peak occurring at a lag of 30–50 days, followed by a second peak at 75–80 days. This bimodal pattern suggests an inconsistency in the propagation times of the hydrological effects of drought and heatwave. Building upon our earlier findings (Figures 6 and 7), we posit that the first peak likely corresponds to the more immediate runoff deficit induced by the drought component, while the second peak reflects the delayed streamflow loss attributable to the prolonged impacts of the associated heatwave.

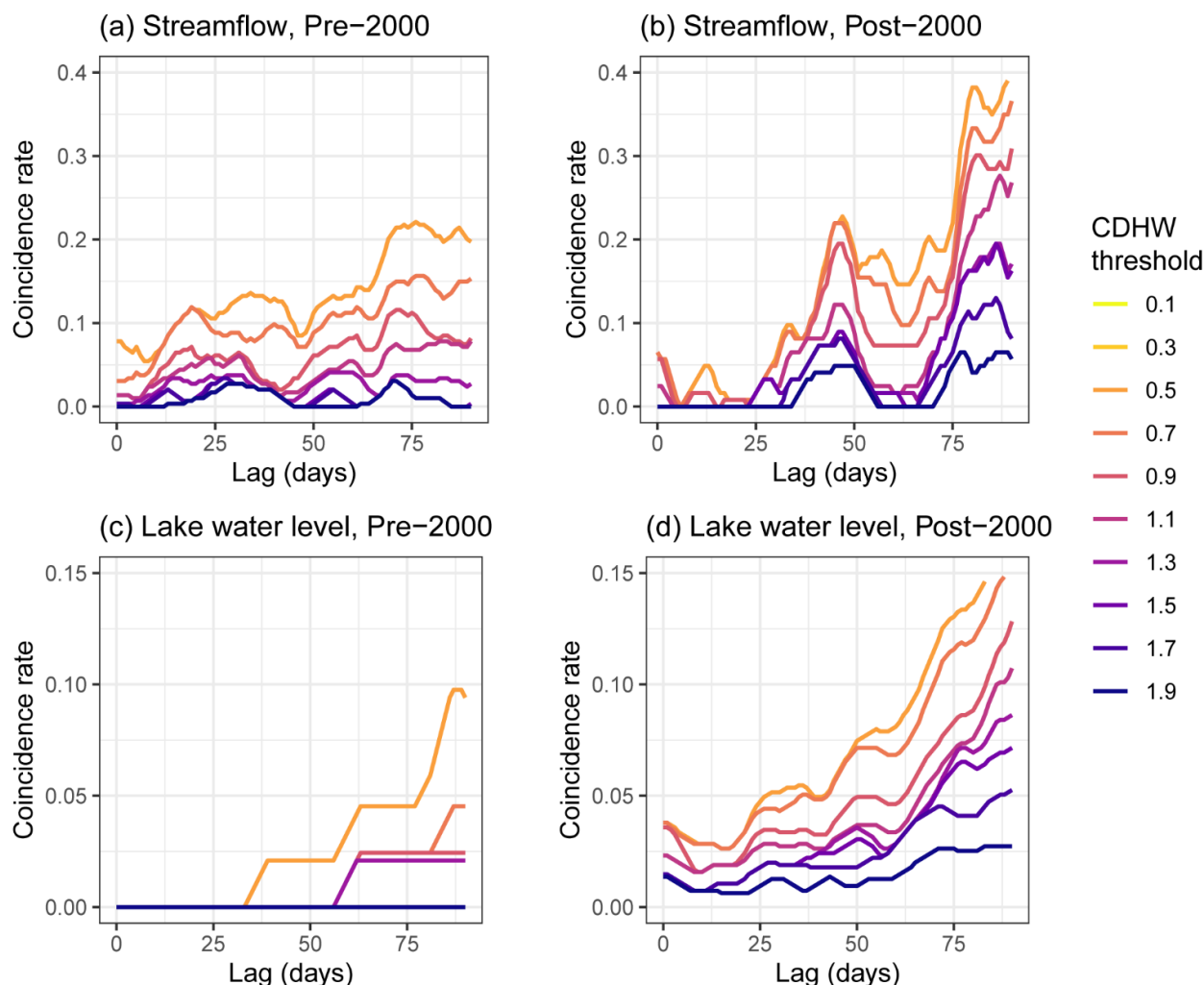


Figure 8. Sensitivity of hydrological drought coincidence to CDHW severity. The lagged coincidence rate between (a,b) streamflow drought and (c,d) lake water drought for CDHW of varying severity thresholds. The left column (a,c) represents the pre-2000 period, and the right column (b,d) the post-2000 period.

The sensitivity of lake water drought to CDHW shared similarities but also key differences (Figure 8c,d). Unlike streamflow, the lake's response did not exhibit a bimodal pattern. As the terminal integrator in the hazard propagation chain, the lake's response to climatic extremes is more blended and attenuated, resulting in a coincidence rate that monotonically increases with lag. In the pre-2000 period, no clear response could be detected for several of the higher severity thresholds.

In conclusion, the hydrological lagged impacts of CDHW are not only present but are highly sensitive to the events' severity. The emergence of a bimodal response in streamflow underscores the distinct and sequential propagation of drought and heatwave effects through the watershed, a dynamic that is amplified under recent warming and for more severe compound events.

4. Discussion

4.1. Increasing Threat of CDHW

Our analysis provides robust empirical evidence for a paradigmatic shift in the CDHW regime. This evidence is constituted by: (1) statistically significant increasing trends in frequency, severity, and intensity across the basin; (2) a fundamental alteration in the statistical distributions of these metrics post-2000; and (3) the spatially heterogeneous pattern

of amplification, which rules out a uniform random fluctuation. The results presented in Section 3.1 demonstrate significant increases in the frequency, severity, and intensity of CDHW events, with a pronounced acceleration post-2000 (Figures 2 and 3). This intensification is not merely a matter of degree but represents a fundamental alteration in the statistical properties of these events, characterized by a shift in probability density functions toward higher values and the emergence of a secondary peak in intensity distributions (Figure 3). Our findings align with global studies documenting an increase in compound hot-dry events [17,35], but we further reveal that in a monsoonal basin, this warming-driven intensification is not uniform but is instead modulated by regional physiography, leading to the observed meridional gradient and specific spatial hotspots.

The post-2000 surge in CDHW events coincides with a regime shift in the East Asian summer monsoon, characterized by a weakening of the monsoon flow and more frequent stagnation of high-pressure systems over the region. This synoptic configuration favors prolonged periods of reduced precipitation and increased solar radiation, creating ideal conditions for the initiation and persistence of CDHW [53]. Therefore, the increasing threat of CDHW in the PLB is not a simple linear response to global warming but a consequence of the interplay between large-scale circulation changes and regional land–atmosphere processes, which collectively have pushed the basin’s climate system into a new state where high-intensity compound extremes have become the new normal in autumn [54].

The post-2000 surge in CDHW events coincides with and is likely driven by documented shifts in large-scale atmospheric circulation over East Asia [55]. A key driver is the persistent anomalous high-pressure system (e.g., a strengthened and westward-extended Western Pacific Subtropical High, WPSH) [56] and a concurrent weakening of the East Asian summer monsoon [57]. This synoptic configuration favors prolonged atmospheric stability, reduced cloud cover, and subsidence, which collectively suppress convective precipitation (leading to drought initiation) and promote increased solar radiation and adiabatic warming (intensifying heatwaves). Furthermore, the initial soil moisture deficit from the precipitation shortage reduces latent heat flux and increases sensible heating, positive land–atmosphere feedback that further amplifies near-surface temperatures, tightly coupling the drought and heatwave evolution [58]. This interplay between large-scale circulation changes and regional land–atmosphere processes has pushed the basin’s climate system into a state more conducive to high-intensity compound extremes.

4.2. Lagged Influence on Hydrological Drought

A central finding of this research is the quantification of how intensified CDHW translate into more severe and protracted hydrological droughts through lagged effects (Section 3.2). Our ECA reveals that the immediate (lag 0) hydrological response to CDHW is modest, but the trigger coincidence rate increases substantially at seasonal timescales (lags of 40–90 days), especially in the post-2000 period (Figure 5). Crucially, by deconstructing CDHW into their constituent drivers (Figures 6 and 7), we identified that this enhanced lagged impact is primarily governed by the persistent hydrological signature of the heatwave component, whereas the drought component exerts a more immediate but rapidly decaying influence.

This finding can be explained from an energy and evapotranspiration perspective. Meteorological drought (precipitation deficit) impacts streamflow primarily through a reduction in direct runoff and shallow subsurface flow, processes that operate on timescales of days to weeks, explaining the immediate but short-lived signal of standalone droughts [59]. In contrast, a heatwave imposes a prolonged hydrological stress by fundamentally altering the watershed’s energy balance [60]. The excessive atmospheric heat demand, represented by high vapor pressure deficit, drives a continuous and intense depletion of soil moisture

from deeper soil layers and groundwater. This process sustains evapotranspiration at the cost of reducing baseflow that sustains river discharge and lake levels over seasonal timescales [61]. In a CDHW event, the initial drought sets up a dry state, and the concurrent heatwave then acts as an atmospheric pump, efficiently and persistently draining the watershed's moisture reserves. This explains the observed bimodal response in streamflow for high-severity CDHW (Figure 8a,b): the first peak (30–50 days) likely represents the integrated response to the initial precipitation deficit and rapid soil moisture drainage, while the second, more pronounced peak (75–80 days) reflects the delayed and cumulative impact of heat-driven water losses from the deeper and slower components of the hydrological system.

For the lake itself, the response is even more lagged and attenuated (Figures 5b and 8c,d). As the terminal integrator of the entire basin, Poyang Lake's level reflects the spatially and temporally aggregated hydrological response. The absence of a bimodal pattern and the monotonic increase in coincidence rate with lag underscore that the lake effectively filters out the high-frequency, immediate signals, while integrating the long-term, cumulative water deficits propagated through the river network and groundwater. The finding that post-2000 coincidence rates surpass pre-2000 rates for all lags in the lake system underscores that recent warming has imposed a basin-wide, persistent hydrological stress that is fundamentally altering the lake's water budget over extended periods [62].

4.3. Implications, Limitations and Future Scope

The implications of our findings are threefold and extend beyond the PLB to other monsoonal freshwater systems. First, the regime shift in CDHW characteristics implies that the traditional, univariate approach to extreme event risk assessment is no longer sufficient. Water resource management and drought early warning systems must evolve to account for the compounding nature of droughts and heatwaves and their non-linear, lagged impacts on water availability [63]. Second, the dominance of heatwaves in driving the lagged hydrological impact reveals a previously underappreciated vulnerability. It suggests that even in a precipitation-rich basin, a hot drought can inflict more severe and long-lasting hydrological consequences than a pure precipitation drought, a paradigm that challenges conventional water planning [64]. Third, the spatial heterogeneity of CDHW amplification calls for targeted adaptation strategies. Hotspots in the northern sub-basins, which are major contributors to the lake's water supply, require prioritized interventions.

This study has several limitations. Firstly, our analysis establishes robust statistical linkages but does not fully resolve the physical processes using a land surface model. Future work should integrate a physically based model to explicitly partition the energy and water fluxes during CDHW and to quantify the relative contributions of dynamic vegetation and human water management (e.g., reservoir operations) to the observed hydrological responses. Secondly, the use of a fixed 90-day window for index calculation, while climatically justified, may not fully capture the variable memory of the land surface. Experiments with time-varying scales could provide further insights. Finally, the projection of future CDHW risks and their hydrological impacts under different emission scenarios using high-resolution climate models is an essential next step for proactive climate adaptation.

5. Conclusions

This study presents a comprehensive analysis of the spatiotemporal evolution of Compound Drought and Heatwave events and their cascading impacts on hydrological droughts in the Poyang Lake Basin from 1981 to 2016. By employing a multi-metric framework and

event-based coincidence analysis, we move beyond a univariate perspective to uncover the complex and evolving nature of compound extremes in a major monsoonal watershed.

Our findings demonstrate a paradigmatic shift in the CDHW regime post-2000, characterized by a statistically significant increase in the frequency, severity, and intensity of these events. This intensification is not merely an increase in magnitude but represents a fundamental alteration in the statistical properties of CDHW, marked by a shift in their probability distributions toward higher values and a broadening of the seasonal window, with high-intensity events expanding from a concentrated peak in October to encompass September and November.

Through Event coincidence analysis, we revealed that the more intense CDHW of the post-2000 period have led to a significant increase in the triggering of streamflow and lake water droughts, with a particularly pronounced enhancement at seasonal timescales (lags > 40 days). Crucially, by deconstructing the compound events, we identified that this protracted hydrological footprint is primarily governed by the persistent effects of the heatwave component, which imposes a prolonged stress on the watershed's water reserves, in contrast to the more immediate but rapidly decaying influence of the drought component alone. This mechanistic insight is further corroborated by the emergent bimodal lagged response in streamflow for high-severity CDHW, suggesting distinct and sequential propagation pathways for the drought and heatwave impacts through the hydrological system.

In summary, this study provides evidence that recent warming has fundamentally altered the threat profile of compound extremes in the PLB. The escalating CDHW events are not only more frequent and intense but also exert more severe and long-lasting impacts on the basin's hydrology. These findings underscore the critical necessity of integrating compound extreme processes into climate risk assessments and water resource management strategies.

Author Contributions: Conceptualization, N.L. and Y.Y.; methodology, Z.X.; software, Z.X.; validation, Y.Z.; writing—original draft preparation, N.L.; writing—review and editing, Z.X.; visualization, N.L.; supervision, J.W.; project administration, M.M.; funding acquisition, X.Z. All authors have read and agreed to the published version of the manuscript.

Funding: This work was supported by the National Natural Science Foundation of China (42401049), the Jiangxi Provincial Natural Science Foundation (20252BAC200244), the China Postdoctoral Science Foundation (2024M763367), the IWHR Internationally-Oriented Talent for International Academic Leader Program (0203982012), and the Belt and Road Special Foundation of the National Key Laboratory of Water Disaster Prevention (2023490611).

Data Availability Statement: The datasets used and analyzed during the current study are available from the corresponding author upon reasonable request.

Conflicts of Interest: The authors declare no conflicts of interest.

Abbreviations

The following abbreviations are used in this manuscript:

CDHW	Compound drought and heatwave
ECA	Event coincidence analysis
PLB	Poyang Lake Basin
SPI	Standardized Precipitation Index
STI	Standardized Temperature Index
SRI	Standardized Runoff Index
SWI	Standardized Water-level Index

References

1. Liu, J.; Chen, J.; Yin, J.; King, A.D. Time of Emergence of Record-Shattering Compound Heatwave-Extreme Precipitation Events and Their Socio-Economic Exposures. *Geophys. Res. Lett.* **2025**, *52*, e2025GL116884. [\[CrossRef\]](#)
2. Mukherjee, S.; Mishra, A.K. Increase in Compound Drought and Heatwaves in a Warming World. *Geophys. Res. Lett.* **2021**, *48*, e2020GL090617. [\[CrossRef\]](#)
3. Zhang, X.; Gu, X.; Slater, L.J.; Dembélé, M.; Tosunoğlu, F.; Guan, Y.; Liu, J.; Zhang, X.; Kong, D.; Xie, F.; et al. Amplification of Coupled Hot-Dry Extremes over Eastern Monsoon China. *Earth's Future* **2023**, *11*, e2023EF003604. [\[CrossRef\]](#)
4. Yin, J.; Slater, L. Understanding Heatwave-Drought Compound Hazards and Impacts on Socio-Ecosystems. *TIG* **2023**, *1*, 100042. [\[CrossRef\]](#)
5. Min, R.; Gu, X.; Guan, Y.; Zhang, X. Increasing Likelihood of Global Compound Hot-Dry Extremes from Temperature and Runoff during the Past 120 Years. *J. Hydrol.* **2023**, *621*, 129553. [\[CrossRef\]](#)
6. Böhnisch, A.; Felsche, E.; Mittermeier, M.; Poschlod, B.; Ludwig, R. Future Patterns of Compound Dry and Hot Summers and Their Link to Soil Moisture Droughts in Europe. *Earth's Future* **2025**, *13*, e2024EF004916. [\[CrossRef\]](#)
7. Mukherjee, S.; Mishra, A.K.; Ashfaq, M.; Kao, S.-C. Relative Effect of Anthropogenic Warming and Natural Climate Variability to Changes in Compound Drought and Heatwaves. *J. Hydrol.* **2022**, *605*, 127396. [\[CrossRef\]](#)
8. Chen, L.; Chen, X.; Cheng, L.; Zhou, P.; Liu, Z. Compound Hot Droughts over China: Identification, Risk Patterns and Variations. *Atmos. Res.* **2019**, *227*, 210–219. [\[CrossRef\]](#)
9. Liu, J.; Chen, J.; Yin, J.; Su, T.; Xiong, L.; Xia, J. Understanding Compound Extreme Precipitations Preconditioned by Heatwaves over China under Climate Change. *Environ. Res. Lett.* **2024**, *19*, 064077. [\[CrossRef\]](#)
10. Meng, Y.; Hao, Z.; Zhang, Y.; Feng, S. The 2022-like Compound Dry and Hot Extreme in the Northern Hemisphere: Extremeness, Attribution, and Projection. *Atmos. Res.* **2023**, *295*, 107009. [\[CrossRef\]](#)
11. Li, C.; Gu, X.; Bai, W.; Slater, L.J.; Li, J.; Kong, D.; Liu, J.; Li, Y. Asymmetric Response of Short- and Long-Duration Dry Spells to Warming during the Warm-Rain Season over Eastern Monsoon China. *J. Hydrol.* **2021**, *603*, 127114. [\[CrossRef\]](#)
12. Sharma, S.; Mujumdar, P.P. Spatial Synchrony, Temporal Clustering and Dominant Driver of Streamflow Droughts in Peninsular India. *Environ. Res. Lett.* **2024**, *19*, 074056. [\[CrossRef\]](#)
13. Wang, H.; Zhang, G.; Zhang, S.; Shi, L.; Su, X.; Song, S.; Feng, K.; Zhang, T.; Fu, X. Development of a Novel Daily-Scale Compound Dry and Hot Index and Its Application across Seven Climatic Regions of China. *Atmos. Res.* **2023**, *287*, 106700. [\[CrossRef\]](#)
14. Liu, Y.; Zhu, Y.; Ren, L.; Singh, V.P.; Yong, B.; Jiang, S.; Yuan, F.; Yang, X. Understanding the Spatiotemporal Links Between Meteorological and Hydrological Droughts from a Three-Dimensional Perspective. *JGR Atmos.* **2019**, *124*, 3090–3109. [\[CrossRef\]](#)
15. Ullah, I.; Zeng, X.-M.; Mukherjee, S.; Aadhar, S.; Mishra, A.K.; Syed, S.; Ayugi, B.O.; Iyakaremye, V.; Lv, H. Future Amplification of Multivariate Risk of Compound Drought and Heatwave Events on South Asian Population. *Earth's Future* **2023**, *11*, e2023EF003688. [\[CrossRef\]](#)
16. François, B.; Vrac, M. Time of Emergence of Compound Events: Contribution of Univariate and Dependence Properties. *Nat. Hazards Earth Syst. Sci.* **2023**, *23*, 21–44. [\[CrossRef\]](#)
17. Wang, C.; Li, Z.; Chen, Y.; Ouyang, L.; Li, Y.; Sun, F.; Liu, Y.; Zhu, J. Drought-Heatwave Compound Events Are Stronger in Drylands. *Weather Clim. Extrem.* **2023**, *42*, 100632. [\[CrossRef\]](#)
18. Wang, Y.; Wang, J.; Gong, D.; Ding, M.; Zhong, W.; Deng, M.; Kang, Q.; Ding, Y.; Liu, Y.; Zhang, J. Spatiotemporal Heterogeneity and Zonal Adaptation Strategies for Agricultural Risks of Compound Dry and Hot Events in China's Middle Yangtze River Basin. *Remote Sens.* **2025**, *17*, 2892. [\[CrossRef\]](#)
19. Zhang, G.; Zhang, S.; Wang, H.; Yew Gan, T.; Su, X.; Wu, H.; Shi, L.; Xu, P.; Fu, X. Evaluating Vegetation Vulnerability under Compound Dry and Hot Conditions Using Vine Copula across Global Lands. *J. Hydrol.* **2024**, *631*, 130775. [\[CrossRef\]](#)
20. Donges, J.F.; Schleussner, C.-F.; Siegmund, J.F.; Donner, R.V. Event Coincidence Analysis for Quantifying Statistical Interrelationships between Event Time Series: On the Role of Flood Events as Triggers of Epidemic Outbreaks. *Eur. Phys. J. Spec. Top.* **2016**, *225*, 471–487. [\[CrossRef\]](#)
21. Siegmund, J.F.; Siegmund, N.; Donner, R.V. CoinCalc—A New R Package for Quantifying Simultaneities of Event Series. *Comput. Geosci.* **2017**, *98*, 64–72. [\[CrossRef\]](#)
22. Xing, Z.; Wei, J.; Li, Y.; Zhang, X.; Ma, M.; Yi, P.; Ju, Q.; Laux, P.; Kunstmann, H. Disentangling the Spatially Combined and Temporally Lagged Influences of Climate Oscillations on Seasonal Droughts in the East Asian Monsoon Influenced Poyang Lake Basin. *Atmos. Res.* **2024**, *310*, 107603. [\[CrossRef\]](#)
23. Wei, J.; Knoche, H.R.; Kunstmann, H. Contribution of Transpiration and Evaporation to Precipitation: An ET-Tagging Study for the Poyang Lake Region in Southeast China. *JGR Atmos.* **2015**, *120*, 6845–6864. [\[CrossRef\]](#)
24. Li, Y.; Zhang, Q.; Tao, H.; Yao, J. Integrated Model Projections of Climate Change Impacts on Water-Level Dynamics in the Large Poyang Lake (China). *Hydrol. Res.* **2021**, *52*, 43–60. [\[CrossRef\]](#)
25. Zhou, H.; Zhou, W.; Liu, Y.; Yuan, Y.; Huang, J.; Liu, Y. Meteorological Drought Migration in the Poyang Lake Basin, China: Switching among Different Climate Modes. *J. Hydrometeorol.* **2020**, *21*, 415–431. [\[CrossRef\]](#)

26. McKee, T.B.; Doesken, N.J.; Kleist, J. The Relationship of Drought Frequency and Duration to Time Scales. In Proceedings of the Eighth Conference on Applied Climatology, Anaheim, CA, USA, 17–22 January 1993; pp. 179–184.

27. Han, J.; Singh, V.P.; Kwon, H.-H.; Kim, T.-W. Forecasting Compound Drought-Heatwaves Using Burg Entropy Spectral Analysis with Multi-Frequency Resolutions. *J. Hydrol.* **2025**, *658*, 133166. [\[CrossRef\]](#)

28. Hu, Y.; Wang, W.; Wang, P.; Teuling, A.J.; Zhu, Y. Spatial-Temporal Variations and Drivers of the Compound Dry-Hot Event in China. *Atmos. Res.* **2024**, *299*, 107160. [\[CrossRef\]](#)

29. Dong, N.; Yang, M.; Yu, Z.; Wei, J.; Yang, C.; Yang, Q.; Liu, X.; Lei, X.; Wang, H.; Kunstmann, H. Water Resources Management in a Reservoir-Regulated Basin: Implications of Reservoir Network Layout on Streamflow and Hydrologic Alteration. *J. Hydrol.* **2020**, *586*, 124903. [\[CrossRef\]](#)

30. Li, Y.; Zhang, Q.; Tan, Z.; Yao, J. On the Hydrodynamic Behavior of Floodplain Vegetation in a Flood-Pulse-Influenced River-Lake System (Poyang Lake, China). *J. Hydrol.* **2020**, *585*, 124852. [\[CrossRef\]](#)

31. Zhang, Q.; Xiao, M.; Singh, V.P.; Wang, Y. Spatiotemporal Variations of Temperature and Precipitation Extremes in the Poyang Lake Basin, China. *Theor. Appl. Clim.* **2016**, *124*, 855–864. [\[CrossRef\]](#)

32. Zhang, Y.; Qin, B.; Zhu, G.; Song, C.; Deng, J.; Xue, B.; Gong, Z.; Wang, X.; Wu, J.; Shi, K.; et al. Importance and Main Ecological and Environmental Problems of Lakes in China. *Chin. Sci. Bull.* **2022**, *67*, 3503–3519. [\[CrossRef\]](#)

33. Muñoz-Sabater, J.; Dutra, E.; Agustí-Panareda, A.; Albergel, C.; Arduini, G.; Balsamo, G.; Boussetta, S.; Choulga, M.; Harrigan, S.; Hersbach, H.; et al. ERA5-Land: A State-of-the-Art Global Reanalysis Dataset for Land Applications. *Earth Syst. Sci. Data* **2021**, *13*, 4349–4383. [\[CrossRef\]](#)

34. Cannon, A.J.; Sobie, S.R.; Murdock, T.Q. Bias Correction of GCM Precipitation by Quantile Mapping: How Well Do Methods Preserve Changes in Quantiles and Extremes? *J. Clim.* **2015**, *28*, 6938–6959. [\[CrossRef\]](#)

35. Wu, H.; Su, X.; Singh, V.P. Blended Dry and Hot Events Index for Monitoring Dry-Hot Events over Global Land Areas. *Geophys. Res. Lett.* **2021**, *48*, e2021GL096181. [\[CrossRef\]](#)

36. Xu, Y.; Zhang, X.; Wang, X.; Hao, Z.; Singh, V.P.; Hao, F. Propagation from Meteorological Drought to Hydrological Drought under the Impact of Human Activities: A Case Study in Northern China. *J. Hydrol.* **2019**, *579*, 124147. [\[CrossRef\]](#)

37. Yue, S.; Sheng, X.; Yang, F. Spatiotemporal Evolution and Meteorological Triggering Conditions of Hydrological Drought in the Hun River Basin, NE China. *Nat. Hazards Earth Syst. Sci.* **2022**, *22*, 995–1014. [\[CrossRef\]](#)

38. Spinoni, J.; Barbosa, P.; Buccignani, E.; Cassano, J.; Cavazos, T.; Christensen, J.H.; Christensen, O.B.; Coppola, E.; Evans, J.; Geyer, B.; et al. Future Global Meteorological Drought Hot Spots: A Study Based on CORDEX Data. *J. Clim.* **2020**, *33*, 3635–3661. [\[CrossRef\]](#)

39. Vicente-Serrano, S.M.; Beguería, S.; López-Moreno, J.I. A Multiscalar Drought Index Sensitive to Global Warming: The Standardized Precipitation Evapotranspiration Index. *J. Clim.* **2010**, *23*, 1696–1718. [\[CrossRef\]](#)

40. Xing, Z.; Yu, Z.; Wei, J.; Zhang, X.; Ma, M.; Yi, P.; Ju, Q.; Wang, J.; Laux, P.; Kunstmann, H. Lagged Influence of ENSO Regimes on Droughts over the Poyang Lake Basin, China. *Atmos. Res.* **2022**, *275*, 106218. [\[CrossRef\]](#)

41. Liu, Z.; Lu, G.; He, H.; Wu, Z.; He, J. A Conceptual Prediction Model for Seasonal Drought Processes Using Atmospheric and Oceanic Standardized Anomalies: Application to Regional Drought Processes in China. *Hydrol. Earth Syst. Sci.* **2018**, *22*, 529–546. [\[CrossRef\]](#)

42. Liu, Z.; Lu, G.; He, H.; Wu, Z.; He, J. Understanding Atmospheric Anomalies Associated with Seasonal Pluvial-Drought Processes Using Southwest China as an Example. *JGR Atmos.* **2017**, *122*, 12210–12225. [\[CrossRef\]](#)

43. Shukla, S.; Wood, A.W. Use of a Standardized Runoff Index for Characterizing Hydrologic Drought. *Geophys. Res. Lett.* **2008**, *35*, 2007GL032487. [\[CrossRef\]](#)

44. Wilcox, R.R. Theil-Sen Estimator. In *Introduction to Robust Estimation and Hypothesis Testing*; Academic Press: Amsterdam, The Netherlands, 2005; pp. 423–427.

45. Ross, G.J. Parametric and Nonparametric Sequential Change Detection in R: The Cpm Package. *J. Stat. Softw.* **2015**, *66*, 1–20. [\[CrossRef\]](#)

46. Saharwardi, M.S.; Hassan, W.U.; Dasari, H.P.; Gandham, H.; Ag, P.; Hoteit, I. Rising Occurrence of Compound Droughts and Heatwaves in the Arabian Peninsula Linked to Large-Scale Atmospheric Circulations. *Sci. Total Environ.* **2025**, *978*, 179433. [\[CrossRef\]](#)

47. Benz, S.A.; Irvine, D.J.; Rau, G.C.; Bayer, P.; Menberg, K.; Blum, P.; Jamieson, R.C.; Griebler, C.; Kurylyk, B.L. Global Groundwater Warming Due to Climate Change. *Nat. Geosci.* **2024**, *17*, 545–551. [\[CrossRef\]](#)

48. Baez-Villanueva, O.M.; Zambrano-Bigiarini, M.; Miralles, D.G.; Beck, H.E.; Siegmund, J.F.; Alvarez-Garreton, C.; Verbist, K.; Garreaud, R.; Boisier, J.P.; Galleguillos, M. On the Timescale of Drought Indices for Monitoring Streamflow Drought Considering Catchment Hydrological Regimes. *Hydrol. Earth Syst. Sci.* **2024**, *28*, 1415–1439. [\[CrossRef\]](#)

49. He, X.; Sheffield, J. Lagged Compound Occurrence of Droughts and Pluvials Globally over the Past Seven Decades. *Geophys. Res. Lett.* **2020**, *47*, e2020GL087924. [\[CrossRef\]](#)

50. Zhang, Y.; Hong, S.; Liu, D.; Piao, S. Susceptibility of Vegetation Low-Growth to Climate Extremes on Tibetan Plateau. *Agric. For. Meteorol.* **2023**, *331*, 109323. [\[CrossRef\]](#)

51. Siegmund, J.F.; Sanders, T.G.M.; Heinrich, I.; Van Der Maaten, E.; Simard, S.; Helle, G.; Donner, R.V. Meteorological Drivers of Extremes in Daily Stem Radius Variations of Beech, Oak, and Pine in Northeastern Germany: An Event Coincidence Analysis. *Front. Plant Sci.* **2016**, *7*, 733. [\[CrossRef\]](#)

52. Miao, L.; Yu, Z.; Zhu, X.; Agathokleous, E.; Bao, G.; Iqbal, P.; Liu, Q. Grassland Growth Response to Drought in Dryland Inner Mongolia: Insights from a Two-Decade Analysis. *Environ. Res. Lett.* **2025**, *20*, 074038. [\[CrossRef\]](#)

53. Wang, L.; Huang, G.; Chen, W.; Wang, T. Super Drought under Global Warming: Concept, Monitoring Index, and Validation. *Bull. Am. Meteorol. Soc.* **2023**, *104*, E943–E969. [\[CrossRef\]](#)

54. Hao, Z.; Chen, Y.; Feng, S.; Liao, Z.; An, N.; Li, P. The 2022 Sichuan-Chongqing Spatio-Temporally Compound Extremes: A Bitter Taste of Novel Hazards. *Sci. Bull.* **2023**, *68*, 1337–1339. [\[CrossRef\]](#)

55. Wang, L.; Huang, G.; Chen, W.; Wang, T.; Chotamonsak, C.; Limsakul, A. Decadal Background for Active Extreme Drought Episodes in the Decade of 2010–2019 over Southeastern Mainland Asia. *J. Clim.* **2022**, *35*, 2785–2803. [\[CrossRef\]](#)

56. Li, Z.; Yang, Q.; Yuan, D.; Lu, E.; Ma, Z. Causes of a Typical Southern Flood and Northern Drought Event in 2015 over Eastern China. *Adv. Atmos. Sci.* **2023**, *40*, 2092–2107. [\[CrossRef\]](#)

57. Zhang, R.; Zhou, W.; Tian, W.; Zhang, Y.; Zhang, J.; Luo, J. A Stratospheric Precursor of East Asian Summer Droughts and Floods. *Nat. Commun.* **2024**, *15*, 247. [\[CrossRef\]](#)

58. Benson, D.O.; Dirmeyer, P.A. Characterizing the Relationship between Temperature and Soil Moisture Extremes and Their Role in the Exacerbation of Heat Waves over the Contiguous United States. *J. Clim.* **2021**, *34*, 2175–2187. [\[CrossRef\]](#)

59. Zhang, D.; Liu, X.; Li, X.; Wang, K.; Fan, X.; Yuan, C. Propagation from Atmospheric Water Deficit to Lake Drought in Lake Basins Across China: Implications for Lake Drought Management. *Water Resour. Res.* **2025**, *61*, e2024WR039641. [\[CrossRef\]](#)

60. Zhang, K.; Zhan, Y.; Zuo, Z.; Bu, L.; Chang, M.; Qiao, L. Land-Air Coupling Exacerbates the Future Risk of Concurrent Daytime-Nighttime Hot Extremes. *Sci. China Earth Sci.* **2025**, *68*, 1261–1273. [\[CrossRef\]](#)

61. Chen, H.; Fan, L.; Li, Q.; Wang, Y.; Liu, D.; Zhao, F. Future Climate Change Exacerbates Streamflow Depletion in the Wei River Basin, China. *J. Hydrol.* **2025**, *663*, 134146. [\[CrossRef\]](#)

62. Cheng, X.; Wang, S.; Chen, J.; AghaKouchak, A. Global Assessment and Hotspots of Lake Drought. *Commun. Earth Environ.* **2025**, *6*, 308. [\[CrossRef\]](#)

63. Ma, F.; Yuan, X.; Liu, X. Intensification of Drought Propagation over the Yangtze River Basin under Climate Warming. *Int. J. Climatol.* **2023**, *43*, 5640–5661. [\[CrossRef\]](#)

64. Martinez-Villalobos, C.; Fu, D.; Loikith, P.C.; Neelin, J.D. Accelerating Increase in the Duration of Heatwaves under Global Warming. *Nat. Geosci.* **2025**, *18*, 716–723. [\[CrossRef\]](#)

Disclaimer/Publisher's Note: The statements, opinions and data contained in all publications are solely those of the individual author(s) and contributor(s) and not of MDPI and/or the editor(s). MDPI and/or the editor(s) disclaim responsibility for any injury to people or property resulting from any ideas, methods, instructions or products referred to in the content.